Influence of liquid crystalline phases on the tunability of a random laser

José Trull,[1] Josep Salud,[2] Sergio Diez-Berart,[2] and David O. López[2,*]

[1]*Grup de Dinàmica no Linial, Òptica no Linial i Lasers (DONLL), Departament de Física, E.S.E.I.A.A.T. Universitat Politècnica de Catalunya, Colom 11, E- 08222 Terrassa, Spain*

[2]*Grup de Propietas Físiques dels Materials (GRPFM), Departament de Física, E.T.S.E.I.B. Universitat Politècnica de Catalunya, Diagonal 647, E-08028 Barcelona, Spain*

(Received 6 March 2017; published 30 May 2017)

In this paper, we report the temperature behavior of an optimized disordered photonic system-based liquid crystal by means of heat capacity and refractive index measurements. The scattering system is formed by a porous borosilicate glass random matrix (about 60%) infiltrated with a smectogenic liquid crystal (about 16%) and a small amount of laser dye (0.1%). The rest of the scattering system is about 24% air, giving rise to a high refractive index contrast scattering system. Such a system has the functionality to change the refractive index contrast with temperature due to the liquid crystal temperature behavior. The system, optically pumped by the second harmonic of a Q-switched Nd:YAG pulsed laser working at 532 nm, exhibits random laser action, the threshold of which depends upon the liquid crystalline mesophase. Temperatures of existence of the smectic-B phase correspond to the most optimized random laser. In such a mesophase, the transport mean free path has been determined as about 16 μm in a coherent backscattering experiment.

DOI: 10.1103/PhysRevE.95.052704

I. INTRODUCTION

Disordered dielectric materials in which the propagation of light is strongly scattered are denoted random photonic systems. The possibility of optical amplification via stimulated emission can occur without an amplifying laser cavity. Letokhov and co-workers [1,2] theoretically predicted laser emission in a diffusive material as a consequence of multiple scattering of light in the late 1960s. This phenomenon is known as random lasing [3,4] and was firstly observed experimentally in laser crystal powders [5] and later in several disordered materials such as microparticles in laser dye solutions [6], semiconductor powders [7], and even in biological tissues [8,9].

One of the most important material properties in random photonic systems is the transport mean free path ℓ defined as the average distance traveled by a wave before the direction of propagation is randomized. Multiple light scattering regime requires that $\ell \ll L$, L being the size of the system. The scattering strength in a disordered photonic material can be easily quantified by means of the so-called disorder parameter $k\ell$ [10], where k is the wave vector of light in vacuum. Anderson localization of light waves [11] is expected for $k\ell \leqslant 1$ and weaker localization occurs for $k\ell > 1$ when the light scattering is assumed to be diffusive. In fact, most of the reported random lasers operate in such a regime with values of the disorder parameter $k\ell$ between 10 and 1000.

A source of controversy is the multiple light scattering feedback caused to obtain a random laser. Cao *et al.* [7] established that the feedback is incoherent when $k\ell \gg 1$ (highly diffusive light scattering regime). In such a regime, the spectral narrowing of the fluorescence band was explained as a phenomenon of amplified spontaneous emission rather than a stimulated one (laser emission). Even so, Cao referred to this phenomenon as random lasing with incoherent feedback [12]. Alternatively, coherent feedback could be possible in the strong scattering regime, when $k\ell$ is close to 1, and light can perform closed-loop paths serving as laser resonators [7,12]. According to Cao [12], only at certain frequencies the wave light interference is constructive giving rise to very narrow discrete peaks in the characteristic emission spectra above threshold. However, Mujumdar et al. [13] performed experiments with several amounts of ZnO powder in a dye solution obtaining samples with $k\ell$ ranging from 35 to 5800 and showing emission spectra comparable to those obtained by Cao *et al.* [7,12]. In such a case, the existence of discrete narrow peaks in the emission spectra was attributed to the generation of very long light paths and was not related to strong scattering regimes and coherent feedback.

Zacharakis *et al.* [14] experimentally studied the coherence of the emission spectra in disordered materials formed by microparticles in laser dye solutions for intermediate diffusive light scattering regimes ($k\ell > 1$) demonstrating that the emitting light was not purely coherent; the result for the temporal coherence was a superposition of Bose-Einstein (characteristic of noncoherent emission) and Poisson statistics (characteristic of classical laser emission). Florescu and John [15] developed a theoretical model according to which it was predicted that for high diffusive light scattering regimes ($k\ell \gg 1$), the light emission above threshold is weakly coherent. However, for low diffusive light scattering regimes ($k\ell$ close to 1) the light emission above threshold is highly coherent. This fact was experimentally observed by Cao *et al.* [16] in ZnO powder disordered systems with a disorder parameter $k\ell$ of about 14. According to Wiersma [17], in a random laser the saturation of the gain above threshold is obtained by the amplification of spontaneously emitted light by means of stimulated emission. Such a mechanism becomes more efficient as the light scattering regime is less diffusive suppressing the fluctuations of intensity and giving rise to emitted light with second-order coherence which is characteristic of coherent feedback.

The refractive index contrast of disordered dielectric media is a crucial parameter that directly influences the scattering

*david.orencio.lopez@upc.edu

strength in random photonic systems. It has been theoretically predicted that a refractive index with a random variation could induce the formation of random resonators trapping the light to be amplified [18]. In intermediate diffusive light scattering regimes ($k\ell > 1$) theoretical approaches satisfy the diffusion approximation and the lasing action depends on the diffusion constant and the transport mean free path, both being dependent on the refractive index contrast [4,19]. It has been recently evidenced how the threshold for lasing decreases as the refractive index contrast of the photonic system increases [20]. The introduction of optical anisotropy in the disordered media could also influence the lasing action [17].

Among the materials that can be optically pumped, organic dyes present low refractive indices, high quantum efficiencies, and they can be easily embedded in a scattering system using an appropriate solvent. After the pioneering work of Wiersma and Cavalieri [21,22] liquid crystals could be used as good solvents for organic dyes with other functionalities related with the optical anisotropy and the variation of the refractive index with temperature or other external stimuli. Random lasers from liquid crystals with organic dyes are relatively scarce [21–26].

In this paper we will present a complete experimental study of random lasers formed by a liquid crystal exhibiting several mesophases as a solvent of a dye infiltrated in a percolating random photonic system. The threshold for laser action is observed to be dependent upon mesophase and is controllable by temperature. Even in the isotropic phase of the liquid crystal in which the regime is assumed to be highly diffusive the laser action is observed at high enough pumping energies. With the purpose to characterize the scattering strength of our disordered system, a tentative value of the disorder parameter $k\ell$ at room temperature is provided by means of coherent backscattering measurements.

The paper is organized as follows. In Sec. II we describe the experimental details. In Sec. III, the results concerning the mesophase behavior of the disordered system, the random laser action at several temperatures, and the coherent backscattering measurements are presented and discussed. Finally, a summary of the most important achieved goals is presented.

II. EXPERIMENTAL DETAILS

A. Material and sample preparation

The sample preparation was made according to the methodology published by Wiersma and Cavalieri [22]. The original idea was to use as a multiple-scattering system a porous disordered structure by pressing glass powder. Here we have used particles of colorless borosilicate glass (hereafter denoted as BG) with arbitrary shape and sizes ranging from 1 to 10 μm pressed under 0.7 GPa giving rise to disks of about 1 cm diameter and about 1.5 mm thick (see Fig. 1). The porosity was estimated to be of about 40% and Fig. 1 shows scanning electron microscope (SEM) views from the top and lateral disk surfaces for two magnifications. The existence of irregular channels, interconnected and truncated in a disordered way, are clearly observed.

An important part in performing a random laser is the gain medium to obtain emission of light and amplification. Among the organic dyes to be optically pumped, the

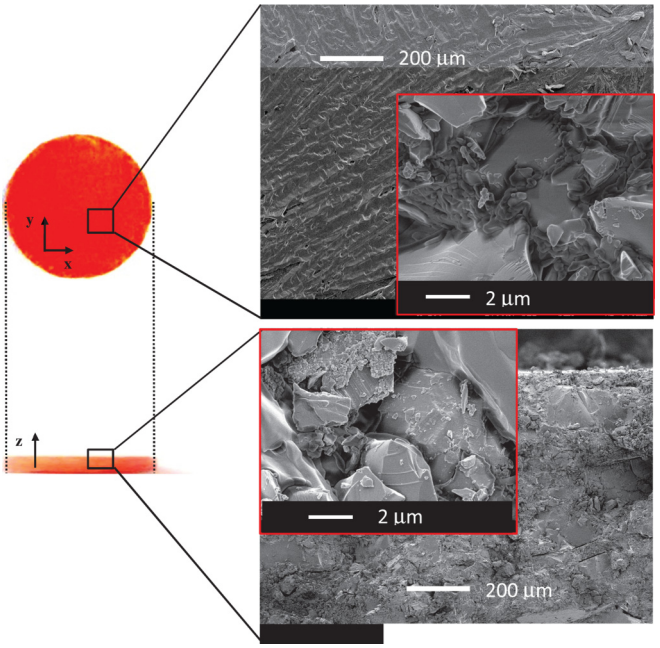

FIG. 1. SEM images of the pressed colorless borosilicate glass as disks of 1 cm diameter and 1.5 mm thickness. View of the disk-surface and lateral-surface at two magnifications.

4-dicyanometylene-2-methyl-6-*p*-dimethylamino-styryl-4*H*-pyran (hereafter denoted as DCM) presents high quantum efficiencies in dissolution. In particular, the compatibility of DCM and calamitic liquid crystals as solvents was proven to be satisfactory [22]. In this work we will use the calamitic liquid crystal compound *n*-(4-*n*-butyloxybenzylidene)-4′-*n*′-octyloaniline ($C_6H_4-NCH-C_6H_4-C_8H_{17}$, hereafter referred to as 4O.8) as a solvent of DCM in several weight fractions of the latter ($X_1 = 1.20 \times 10^{-3}$; $X_2 = 5.15 \times 10^{-3}$; $X_3 = 10.10 \times 10^{-3}$).

Porous disks were immersed in a bath containing the corresponding mixture 4O.8+DCM heated up to 95 °C. Both disk and mixture were kept at this temperature during a period of about 30 min. Filled disks were carefully dried removing the excess of 4O.8+DCM sample from the outer surfaces (see Fig. 1 in which the mixture is visible as shaded regions in the channels) in a procedure similar to other liquid crystal confinement studies performed by some of the authors [27,28]. The estimated filling rate was about 40% of the available porous cavity.

The liquid crystalline behavior of 4O.8+DCM confined to porous disks was characterized by means of heat capacity measurements in a procedure followed in previous studies of liquid crystals confined to porous structures [27–29]. These results together with those related to the refractive index contrast will be presented in Sec. III A and the details of the technique in Sec. II B.

B. Experimental techniques

Heat capacity measurements at atmospheric pressure were performed using a commercial modulated differential scanning calorimeter (DSC-Q2000) from TA Instruments working in

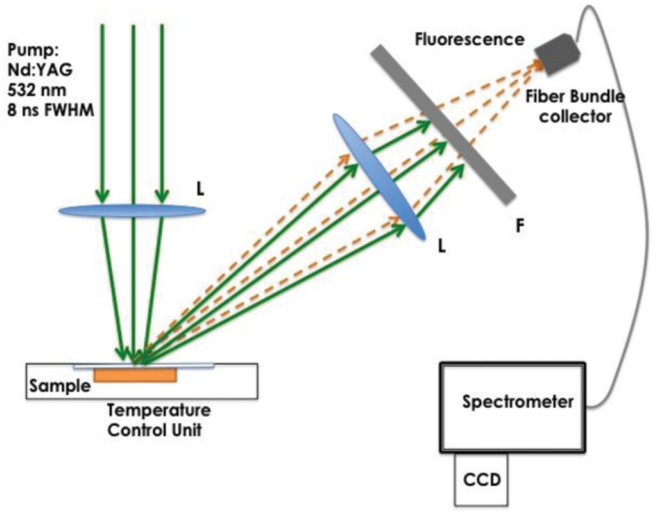

FIG. 2. Schematic setup for random lasing measurements. L and F stand for lens and filter, respectively. The filter was used to block the pump radiation at 532 nm.

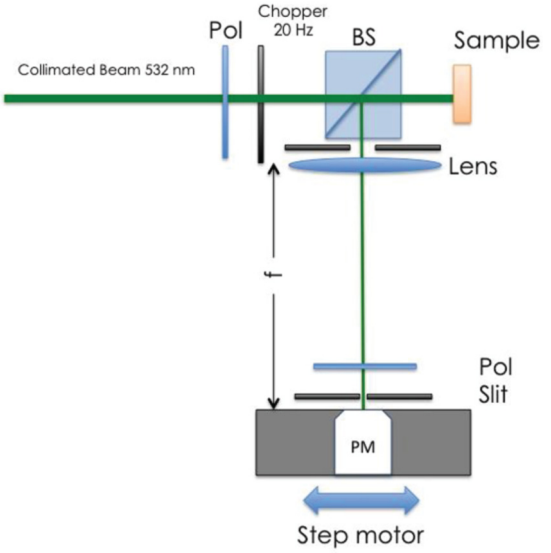

FIG. 3. Experimental configuration for coherent backscattering measurements. BS stands for a nonpolarized cube beam splitter; Pol stands for a linear polarizer; PM stands for a photomultiplier mounted on a translating stage, and the Chopper is used at a frequency of 20 Hz.

the modulated mode. Experimental conditions were adjusted in a way that the imaginary part of the complex heat capacity measurements vanished. On the other hand, as the calorimeter works in the differential mode, the heat capacity of the BG porous disk is directly subtracted from the whole confined system (BG+4O.8+DCM) by putting an empty porous disk in the reference cell. According to this procedure only the heat capacity of the confined 4O.8+DCM mixture is obtained with high resolution [27]. Measurements consist of heating runs at $1\,\mathrm{K\,min^{-1}}$ from 260 up to 360 K and cooling runs at several cooling rates. Modulation parameters (temperature amplitude and oscillation period) were ± 0.5 K and 60 s. A more detailed description of the MDSC technique can be found elsewhere [27,30].

Refractive index measurements were performed independently on 4O.8+DCM mixtures and BG samples by means of a commercial Abbe refractometer (AR-2008) from Kruss Optronic GmbH working with the standard light source of 589 nm in the temperature range of 283–373 K. In optically anisotropic media, both the ordinary (n_o) and extraordinary (n_e) refractive indices were obtained through a Fujiyama 30.5 mm PL filter eyepiece. Calibration was performed with distilled water. The samples were placed between two prisms made of highly refractive glass and the refractive index was obtained by means of the effect of total reflection of the monochromatic light source.

Experiments for random lasing were performed according to the scheme of Fig. 2.

Disk samples were held on a hot stage (TMSG-600) with a temperature controller (TMS-93), both from Linkam and they were optically pumped by the second harmonic of a Q-switched Nd:YAG pulsed laser ($\lambda = 532$ nm, 8 ns FWHM pulse duration) operating in single-shot mode to prevent damage to the sample. The pump beam was focused to a spot of 2 mm diameter (top-hat profile) on the sample surface to access a large gain volume. The spectrum of the fluorescence diffuse emission from the front of the sample surface was recorded, after the pump beam had been filtered out, using a fiber bundle coupled to a spectrometer (Shamrock 303i) using a Peltier-cooled charge-coupled device (CCD) camera (ANDOR DV4204-OE), operated at $-20\,^{\circ}$C for reduced dark noise. The spectral resolution was 0.1 nm and the exposure time of the recorded signal at the CCD was selected to obtain a good signal to noise ratio.

Backscattering experiments were performed using a setup similar to that reported in Ref. [31] and schematically shown in Fig. 3. A highly collimated cw laser beam at a wavelength of 532 nm and with linear s polarization (electric field oriented in the vertical direction) was used to illuminate the sample with a diameter slightly smaller than the sample size. A nonpolarized cube beam splitter was used to shine the incident beam into the sample and to record the backscattered signal in the backward direction. The s-polarized component of the backscattered signal was collected using a lens ($f = 1000$ mm) and a photomultiplier placed at the focal plane and mounted on a closed-loop step motor for lateral displacement. A 200 μm slit was used in front of the photomultiplier tube for angular selection. The selected motor step allowed us to take measurements with a resolution of 0.2 mrad.

III. RESULTS AND DISCUSSION

A. Mesophase behavior and refractive indices

The phase sequence for bulk liquid crystal 4O.8 on heating the sample from room temperature, as reported in the literature [32–34], is the following: crystal (Cry), smectic-B (Sm-B), smectic-A (Sm-A), nematic (N), and isotropic liquid (I). The N phase is the simplest liquid crystalline phase in which the rodlike molecules are anisotropically distributed but on average tend to point in the same direction (no positional order but orientational long-range order). In the Sm-A phase the rodlike molecules maintain the orientational order of

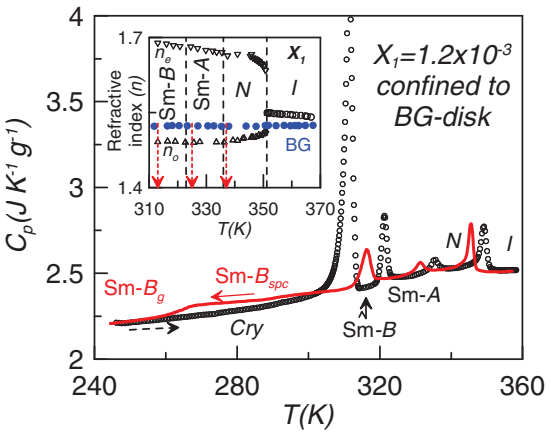

FIG. 4. Heat capacity data as a function of temperature for the confined X_1 sample. Black symbols and continuous curve account for heating and cooling runs, respectively. The inset shows refractive index data as a function of temperature for both X_1 (empty symbols) and borosilicate glass (BG) (full symbols). Arrows in the inset correspond to three representative temperatures of the Sm-*B*, Sm-*A*, and *N* mesophases.

the nematic phase but tend to align in planes or layers perpendicular to the average molecular direction with no particular positional order inside the layer. In the Sm-*B* the rodlike molecules are arranged in a network of hexagons within the layers. All these liquid crystalline phases show optical birefringence.

Laprice and Uhrich [35] reported a glass transition for the Sm-*B* of 4O.8 at $T_g = 175$ K. This has been confirmed by Juszynska *et al.* [36] by adiabatic calorimetry. From x-ray measurements in the Sm-*B*, the hexagonal packing of the molecules within the layers has also been proven. The same authors have also published a more complex polymorphism for bulk 4O.8 where another metastable Sm-*B* phase was identified. Shortly after, Salud *et al.* [37] were unable to observe such a metastable Sm-*B* phase. Probably, the existence or not of such a metastable phase could be a consequence of any impurities in the sample. Anyway, the experiments performed in the present study have been undertaken with the sample of 4O.8 the same as that used by Salud *et al.*

Figure 4 shows the heat capacity of the sample X_1 confined to BG disks as a function of temperature. Black symbols and the red curve correspond to data recorded on heating at a rate of 1 K min^{-1} from 240 up to 360 K and the subsequent cooling at the same rate, respectively. The confined sample on heating shows the same phase sequence for bulk 4O.8 but the phase transition temperatures are downward shifted as observed in Table I where the characteristic transition temperatures for bulk 4O.8 and for the confined X_1 sample are listed. The thermal hysteresis in the Sm-$B \leftrightarrow$ Sm-A, Sm-$A \leftrightarrow N$, and $N \leftrightarrow I$ phase transitions is also evident. It should be stressed that the crystallization of the confined sample is totally inhibited on a cooling run in a way that the Sm-*B* becomes supercooled (Sm-B_{spc}) and finally at a lower temperature exhibits a glass transition, but at temperatures much higher than that reported for bulk 4O.8. These results are identical for the other prepared mixtures 4O.8+DCM proving that the DCM amount is very small and the modifications of transition temperatures are exclusively due to confinement effects. In the next section, only results for the X_1 sample (the lowest content of DCM) will be shown.

The inset of Fig. 4 shows measurements of the refractive index for the X_1 sample as a function of temperature over a wide temperature range. The isotropic phase is nonbirefringent while the other liquid crystalline phases show birefringence that increases as temperature decreases. The refractive index corresponding to the borosilicate glass as a function of temperature is also shown (full symbols), being nearly constant at about 1.52–1.53 over the entire temperature range. It is clear that the X_1 sample and the borosilicate glass show very close refractive indices in the *I* phase and the refractive index contrast is evident for the other liquid crystalline mesophases being maximum at low temperatures in the Sm-*B* phase. This behavior is coincident with the other planned mixtures.

It should be remembered that in our BG disk filled with the X_1 mixture of 4O.8+DCM, about 60% is borosilicate glass while only about 16% is X_1 mixture. The rest, about 24%, is air, giving rise to a multiple-scattering system (BG + X_1 + air). It should be stressed that only the mixture, a minority part of our scattering system, exhibits a refractive index that is strongly temperature dependent.

B. Random laser action in liquid crystalline mesophases

Random laser action was first investigated at three characteristic temperatures, one for each liquid crystalline phase (Sm-*B*, Sm-*A*, and *N*), marked in the inset of Fig. 4 as arrows.

Figure 5 shows the emission intensity peaks for the X_1 mixture of 4O.8+DCM confined to the BG disk at different pumping energies recorded at 313 K (mixture in the Sm-*B* phase). It is clear how the emission peak becomes narrower as the excitation energy increases. The emission intensity peaks labeled *B* and *C* are scaled by a factor of 3 and that labeled *D* by a factor of 12, with the purpose of comparison. The preferential amplification seems to be achieved at frequencies close to the maximum of the broad spontaneous emission peak

TABLE I. Transition temperatures for bulk 4O.8 and for 4O.8+DCM mixture X_1 confined to BG disk.

System	$[T_g]_{\text{Sm-}B}$(K)	$T_{\text{Cry}\rightarrow\text{Sm-}B}$(K)	$T_{\text{Sm-}B\rightarrow\text{Sm-}A}$(K)	$T_{\text{Sm-}A\rightarrow N}$(K)	$T_{N\rightarrow I}$(K)	Reference
Confined X_1	267.3[a]	309.9	320.3	333.2	348.9	This work
Bulk 4O.8		312.5	322.9	336.4	351.2	This work
		310.5[b]	321.1[b]	335.3[b]	351.0[b]	Ref. [35]

[a]Induced by confinement of 4O.8+DCM mixture to BG-porous system.
[b]Data from adiabatic calorimetry.

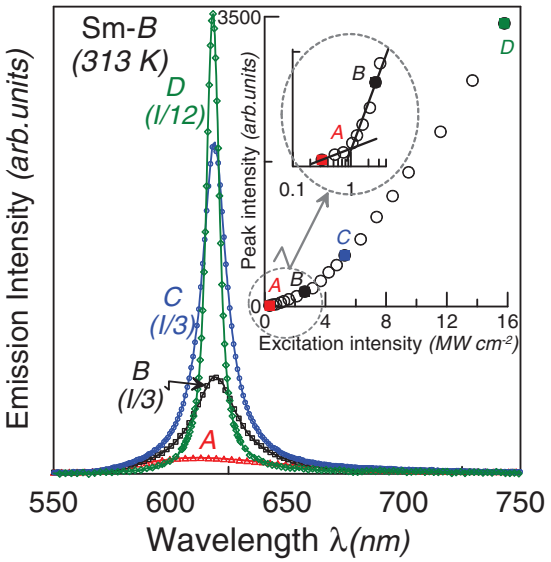

FIG. 5. Emission intensity peaks for the X_1 sample confined to the BG disk at several excitation energies at 313 K with the sample in the Sm-*B* mesophase [A: -Δ- (0.3 MW cm^{-2}); B : -□- (2.6 MW cm^{-2}); C: -o- (5.3 MW cm^{-2}); D: -◇- (15.8 MW cm^{-2})]. The inset shows the intensity at the peak as a function of the excitation intensity.

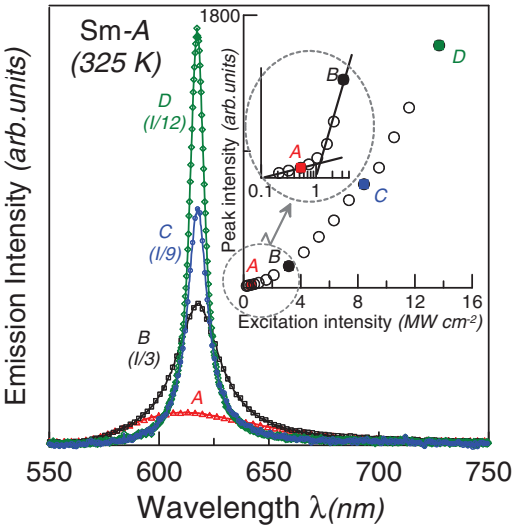

FIG. 6. Emission intensity peaks for the X_1 sample confined to the BG disk at several excitation energies at 325 K with the sample in the Sm-*A* mesophase [A: -Δ- (0.5 MW cm^{-2}); B : -□- (3.2 MW cm^{-2}); C: -o- (8.4 MW cm^{-2}); D: -◇- (15.8 MW cm^{-2})]. The inset shows the intensity at the peak as a function of the excitation intensity.

(labeled *A* in the figure) because they are near the maximum of the gain emission spectrum.

The linewidth of the peak labeled *A*, corresponding to the fluorescence emission at low pump energy, is of the order of 70 nm. The narrower emission peaks were recorded at higher excitation energies; in particular, that labeled *D* corresponds to an excitation intensity of 15.8 MW cm^{-2} with a linewidth less than 7 nm, 10 times narrower than that corresponding to the spontaneous emission band. It should be stressed that although a drastic spectral narrowing is observed as the pump energy increases, discrete narrow peaks emerging on the spontaneous emission band are missing. Such peaks were identified in the past with discrete lasing modes with coherent feedback [7]. However, such identification is controversial and it was suggested that single-shot mode operation with a pulse duration of the order of picoseconds are the ideal conditions (not fulfilled in the present study) to observe discrete peaks with independence of the coherence of the emission spectra [17,38].

The inset of Fig. 5 shows the intensity at the peak of the emission spectrum as a function of the excitation intensity. A lasing threshold behavior is observed as a slope change at an excitation energy of about 1 MW cm^{-2}. The threshold curve evidences a soft threshold as is usually found in other random laser systems. It was suggested that this fact could be due to a strong coupling between the spontaneous emission and the emerging laser modes [39].

Figures 6 and 7 show the behavior of the emission intensity peaks for the same X_1 mixture confined to the BG disk at different pumping energies recorded at two other temperatures: 325 K (mixture in the Sm-*A* phase) and 337 K (mixture in the *N* phase), respectively. At first glance, both figures show a comparable behavior between them and with respect to Fig. 5. However, it is easy to observe how the lasing threshold occurs at higher pumping energies as the temperature increases are about 1.2 MW cm^{-2} for 325 K (Sm-*A* phase) and about 2.3 MW cm^{-2} for 337 K (*N* phase). In addition, the intensity at the emission peak maximum for the same excitation energy is generally smaller as the temperature increases. As an example, the peak labeled *D* (excitation energy of 15.8 MW cm^{-2}) exhibits a peak intensity 2 times smaller at 325 K (Sm-*A* phase) than at 313 K (Sm-*B*) and more than 8 times smaller at 337 K (*N* phase).

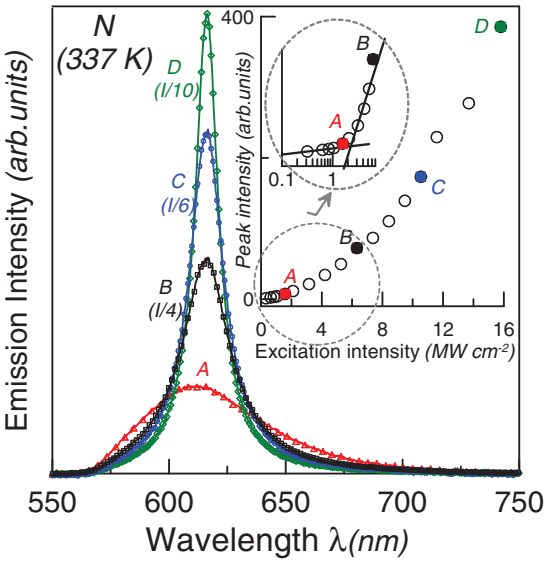

FIG. 7. Emission intensity peaks for the X_1 sample confined to the BG disk at several excitation energies at 337 K with the sample in the *N* mesophase [A: -Δ- (1.6 MW cm^{-2}); B : -□- (6.3 MW cm^{-2}); C: -o- (10.5 MW cm^{-2}); D: -◇- (15.8 MW cm^{-2})]. The inset shows the intensity at the peak as a function of the excitation intensity.

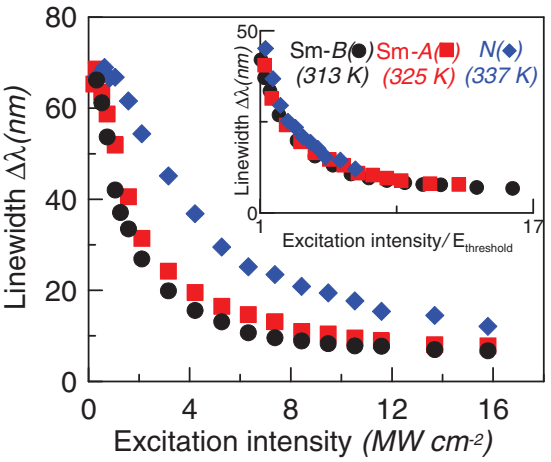

FIG. 8. Linewidth of the emission intensity peaks as a function of the excitation intensity for the sample X_1 at 313 K (filled circles), 325 K (filled squares), and 337 K (filled diamonds). The inset shows the linewidth of the emission intensity peaks as a function of the excitation intensity normalized by that of the laser threshold.

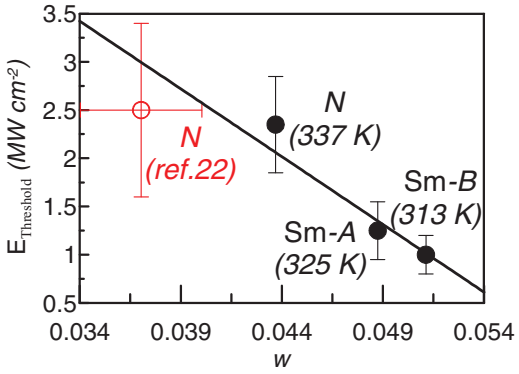

FIG. 9. Laser threshold excitation intensity as a function of the refractive index contrast ratio (w) for sample X_1 at 313, 325, and 337 K. Also included is the symbol corresponding to a closely related system in Ref. [22].

Regarding the linewidth, Fig. 8 shows a comparative evolution of the linewidth with the excitation intensity for the same three temperatures representative of the three liquid crystalline mesophases. It is clearly observed how the linewidth of the emission peaks recorded at temperatures of the smectic mesophases strongly decreases with the pump energy stabilizing at high enough pump energies well above the lasing threshold. The case corresponding to the nematic temperature (337 K) seems to show a smoother linewidth decay with the pump energy. However, it is a cosmetic effect due to the differences in the lasing threshold. Both smectic mesophases exhibit lasing thresholds close to each other but significantly different with respect to that reported for the nematic phase. The inset of Fig. 8 shows how the linewidth as a function of the excitation energy normalized by the energy threshold corresponding to the different liquid crystalline phases collapses onto a master curve showing a comparable decay for excitation energies above lasing threshold. In addition, such a figure also shows how the linewidth in the mesophases tends to the same value for high enough excitation energies.

Random laser action is observed at temperatures corresponding to the several liquid crystalline mesophases but the multiple scattering of light is optimized in the smectic phases in a way such that the lasing becomes easier. The change of the lasing threshold excitation intensity with temperature is evident from the inset of Figs. 5–7 and this modification is only caused by the presence of liquid crystal in our random scattering system as a consequence of the temperature dependence of the refractive index. Figure 9 shows the lasing threshold excitation intensity as a function of the refractive index contrast ratio w, defined by Yi *et al.* [20] as follows:

$$w = \frac{|n_e - n_{\mathrm{BG}}|}{|n_e + n_{\mathrm{BG}}|}, \qquad (1)$$

where n_e and n_{BG} stand for the extraordinary refractive index of the X_1 mixture and the refractive index of the borosilicate glass, respectively.

With the purpose of comparison to other closely related scattering random systems for laser action, we have included the red symbol corresponding to disks of percolated SK11 glass with 7CB liquid crystal+DCM mixture measured under comparable, but not the same, conditions and published by Wiersma and Cavalieri [22]. The error bar is estimated taking into account that only approximate values of refractive indices and pump energy threshold were published by these authors. It is important to mention that the factorization of the refractive index contrast ratio by means of the parameter w does not account for the air content in our system but despite this inconvenience the change of pump energy for the lasing threshold seems to be roughly explained assuming the parameter w. On the other hand, a relationship between the refractive index contrast ratio (w) and the mean free path or the disorder parameter ($k\ell$), in a way that larger values of w imply smaller values of $k\ell$ [20], was suggested.

C. Temperature control of the random laser action

The question now for our scattering system is, will the content of liquid crystal be high enough to avoid laser action at higher temperatures. The basic idea was to select the excitation energy of 15.8 MW cm^{-2}, sufficiently high in relation to the lasing threshold to avoid a chaotic behavior in the emission spectra but not so high as to damage the sample. In Fig. 10(a), we show the emission intensity peaks at 15.8 MW cm^{-2} for the X_1 mixture of 4O.8+DCM confined to the BG disk recorded at several representative temperatures. It is clear how the emission peak becomes wider when temperature moves from 299 up to 357 K (X_1 mixture in the isotropic phase). The peaks corresponding to a laser emission are scaled by the factors shown in the figure with the purpose of comparison. The curve at 357 K corresponds to a broad emission peak characteristic of a fluorescence band (spontaneous emission).

The inset of Fig. 10(a) shows both the linewidth and the peak intensity at maximum as a function of temperature in

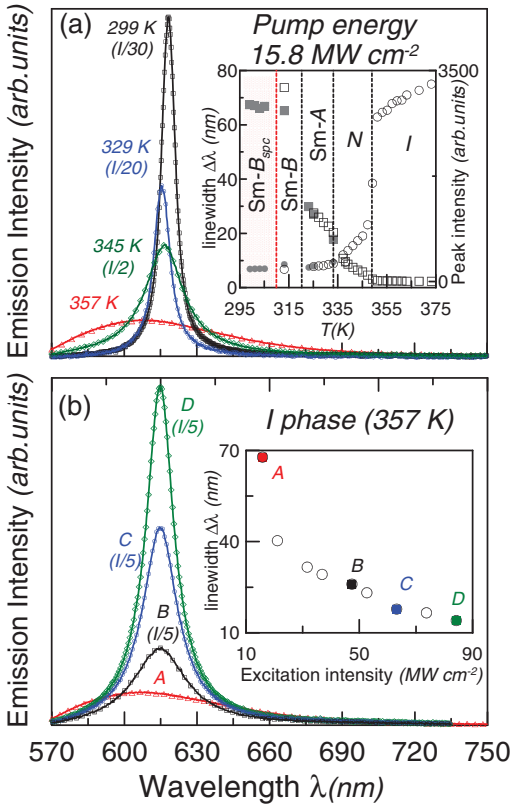

FIG. 10. (a) Emission intensity peaks for the X_1 sample confined to the BG disk at an excitation intensity of 15.8 MW cm^{-2} at several temperatures. The inset shows the linewidth of both the emission intensity peaks (circles) and the peak intensity (squares) as a function of temperature. Empty and full symbols correspond to heating and cooling experiments, respectively. (b) Emission intensity peaks at several excitation energies at 357 K A : -Δ- (15.8 MW cm^{-2}); B : -□- (47 MW cm^{-2}); C : -o- (63 MW cm^{-2}); D: -◇- (84 MW cm^{-2})]. The inset shows the linewidth of the emission intensity peaks as a function of the excitation intenisty.

a wide temperature range. Liquid crystalline phases corresponding to the X_1 mixture confined to the BG disk are clearly delimited by vertical dashed lines representing those phase transition temperatures listed in Table I. It should be stressed that the Cry state is only observed in a first heating experiment from room temperature because the Sm-B mesophase becomes metastable on cooling (Sm-B_{spc}) as indicated in Fig. 10(a) by the red-shaded region), as already discussed previously. Empty and full symbols correspond to heating and cooling run experiments, respectively, and the reproducibility of linewidth data is nicely illustrated. The linewidth evolution with increasing temperature shows a nearly constant value of the order of 7 nm in the Sm-B temperature range and a slight increase in the Sm-A which is accelerated in the N temperature range. A sudden and abrupt increase of the linewidth is observed at the $N \rightarrow I$ phase transition to values higher than 60 nm clearly illustrating the end of laser action. Regarding the peak intensity at maximum, obtained data show that the reproducibility is quite good despite the shot-to-shot fluctuations in the peak intensity being commonly observed in random laser systems [40]. Even so, it can be concluded that the peak intensity at maximum illustrates a saturation at its highest value in the Sm-B temperature range at low temperatures and these values exhibit a nearly continuous decrease as the temperature increases in both the Sm-A and N mesophases up to the $N \rightarrow I$ phase transition.

Figure 10(b) shows the emission spectra recorded at a temperature corresponding to the isotropic state of the X_1 mixture for several excitation energies above 15.8 MW cm^{-2}. The same effect of narrowing the emission peak is observed as in Figs. 5–7. The inset shows how the linewidth becomes narrower as the excitation energy increases but it is clear that to achieve linewidths of the order of 10 nm, the excitation energy has to be higher than 90 MW cm^{-2}. Laser action is possible but at pumping energies so high that the sample is severely damaged.

The control of the laser action by the effect of the temperature dependence of the refractive index attributed to the liquid crystal is really observed despite its low content in the disordered system. It should be remembered that the refractive index of the mixture and that of the BG-porous matrix are nearly coincident (see Fig. 4) at temperatures of the isotropic state but the refractive index contrast with respect to the air inside (24% air has been estimated in our multiple-scattering system) remains giving rise to a very high diffusive light scattering regime ($k\ell \gg 1$).

D. Coherent backscattering measurements

To explore the light scattering regime of our disordered system (sample X_1 confined to BG disks), the disorder parameter $k\ell$ has been tentatively determined in a coherent backscattering experiment with the sample at room temperature. It should be remembered that in our disordered system the most optimized liquid crystalline phase for random laser action is the Sm-B and our methodology consisted in obtaining the supercooled metastable Sm-B phase (Sm-B_{spc}) at room temperature by heating the sample up to the isotropic state followed by a rapid cooling down to room temperature.

In coherent backscattering experiments, the diffuse intensity profile of a sample illuminated by a plane wave is recorded as a function of backscattering angle leading to a coherent backscattering intensity "cone" superimposed on the incoherent background level which is not a function of the transport mean free path. The height of the cone is predicted to be twice the level of the incoherent background in the exact backscattering direction (it is strictly true for circularly polarized light in the helicity preserving channel) [41] as a consequence of the constructive interference of long scattering paths. The width of the "cone" is of the order of $(k\ell)^{-1}$, and for practical calculations on thick enough samples (about or more than 32 transport mean free paths) and parallel-polarized incident light [42] the full width at half maximum (FWHM) of the "cone" is related to the disorder parameter as

$$\mathrm{FWHM} \approx \frac{0.7\,\lambda}{2\pi\ell} = \frac{0.7}{k\ell}. \qquad (2)$$

However, there are some undesirable phenomena that affect the cone shape near the backscattering direction: the sample structure at large depths [41], light absorption at the experimental wavelength [41,43], finite sample size [42,43],

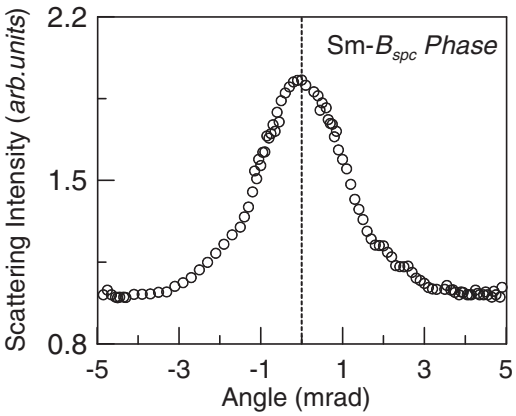

FIG. 11. Coherent backscattering cone for the X_1 sample confined to the BG disk. The sample thickness is 5 mm and was measured at room temperature in the superccoled Sm-B phase (Sm-B_{spc}).

internal reflection [43,44–46], and spurious stray light from sample surface and other components [41].

If the light absorption is present the scattering long paths are reduced and the cusp of the backscattering intensity "cone" appears rounded. In our methodology, the light absorption of the sample at the experiment wavelength (λ) could be only due to the DCM dye which is present in an extremely low amount. The sample thickness was taken to be enough to minimize finite size effects for transport mean free path of about 200 μm or less. The internal reflection effect reduces the width of the backscattering intensity "cone" and the obtained full width at half maximum (FWHM) was corrected by a narrowing factor f_{IR} which takes into account the reflectivity R of the sample-air interface and the effective refractive index of the sample (n_{es}) [46,47]. Equation (2) is applied to calculate the transport mean free path (ℓ) or the disorder parameter ($k\ell$) by taking the corrected full width at half maximum (FWHM/f_{IR}).

Figure 11 shows the measured coherent backscattering intensity cone as a function of the angle with respect to the exact backscattering direction for the supercooled Sm-B phase of the X_1 sample. The full width at half maximum obtained from the figure is 2.5 mrad and the estimated f_{IR} is 0.7 giving rise, through Eq. (2), to a transport mean free path (l) of about 17 μm or a disorder parameter (kl) of 200.

It would be very interesting to compare the obtained transport mean free path with that for other closely related scattering random systems for laser action containing liquid crystals. As cited above, very few works were published for disordered systems containing liquid crystals and those for which the transport mean free path is reported are even scarcer. As far as we know, Wiersma and Cavalieri [22] reported a transport mean free path (l) of 125 μm for SK11 glass with 7CB liquid crystal+DCM mixture in the nematic phase. Assuming that value as well as that reported by us as correct, the disordered system containing liquid crystal proposed by us seems to be closer to other more optimized disordered systems for random laser action like ZnO powder, but with the utility of a random laser exhibiting a temperature control over the excitation energy threshold.

IV. CONCLUDING REMARKS

The idea to design a disordered photonic system based on the capability of liquid crystals to modify the refractive index by means of temperature is not new but the main goal of our study consisted in optimizing such systems for random laser action with an external control by temperature. There are very few studies developing that idea and it seems that the possibility to obtain stronger scattering systems based on liquid crystals was not a priority.

In the present work, we selected the liquid crystal and the powder glass for the same dye (DCM) widely used for others in closely related studies. The optical behavior of a liquid crystal+DCM mixture and the effects of the glass matrix over the mixture when infiltrated were carefully evaluated. The glass matrix was prepared by pressing powder glass at several pressures. Lower pressures than 1.2 GPa [22] were considered to obtain less compact glass matrices to be infiltrated by the mixture. The final result was a complex disordered structure formed by glass (about 60%), liquid crystal (about 16%), a very small amount of DCM (about 0.1%), and air (about 24%).

Random laser action was reported at three temperatures representative of the different liquid crystalline phases. The excitation energy threshold for random laser action clearly depends upon temperature being best optimized for the Sm-B mesophase. Preliminary coherent backscattering measurements lead to a transport mean free path (l) of about 17 μm or a disorder parameter (kl) of 200, about 14 times higher than that reported for ZnO powder [16] but 7 times lower than that for the liquid crystal disordered system published by Wiersma and Cavalieri [22].

The air content in our disordered system provides a high refractive index contrast at every temperature but the temperature dependence of the liquid crystal refractive index allow us to modify the random laser action. This is possible over the liquid crystalline mesophases (Sm-B, Sm-A, and N) for relatively low excitation energy threshold and even at temperatures in the isotropic state but for very high excitation energies causing severe damage to the sample.

The coherence of the emission spectra was not treated in the present study. However, it should be stressed that the light emission above threshold is highly coherent for low diffusive light scattering regimes ($k\ell$ close to 1) as it seems to be the case for ZnO powder [16]. According to Cao [47], in low coherent random lasers the mean frequency of the laser emission is determined only by the frequency of the amplification line and, if this is stable, the emission spectrum is frequency insensitive. In our case, the amplification line is quite stable and the laser emission is nearly frequency insensitive at each temperature.

ACKNOWLEDGMENTS

The authors are grateful for financial support from MINECO Projects No. MAT2015-66208-C3-2-P and No. FIS2015-65998-C2-1-P (MINECO-FEDER). The authors also acknowledge the recognition from the Generalitat de Catalunya of GRPFM and DONLL as consolidated research groups (2014 SGR-190 and 2014 SGR-957).

[1] R. V. Ambartsumyan, N. G. Basov, P. G. Kryukov, and V. S. Letokhov, IEEE J. Quantum Electron. **QE-2**, 442 (1966).
[2] V. S. Letokhov, Sov. Phys. JETP **26**, 835 (1968).
[3] D. S. Wiersma, M. P. van Albada, and A. Lagendijk, Nature **373**, 203 (1995).
[4] D. S. Wiersma and A. Lagendijk, Phys. Rev. E **54**, 4256 (1996).
[5] V. M. Markushev, V. F. Zolin, and Ch. M. Briskina, Sov. J. Quantum Electron. **16**, 281 (1986).
[6] N. M. Lawandy, R. M. Balanchandran, A. S. L. Gomes, and E. Sauvain, Nature **368**, 436 (1994).
[7] H. Cao, Y. G. Zhao, S. T. Ho, E. W. Seelig, Q. H. Wang, and R. P. H. Chang, Phys. Rev. Lett. **82**, 2278 (1999).
[8] M. Siddique, L. Yang, Q. Z. Wang, and R. R. Alfano, Opt. Commun. **117**, 475 (1995).
[9] A. Smuk, E. Lazaro, L. P. Olson, and N. M. Lawandy, Opt. Commun. **284**, 1257 (2011).
[10] D. S. Wiersma, P. Bartolini, A. Lagendijk, and R. Righini, Nature **390**, 671 (1997).
[11] P. W. Anderson, Phys. Rev. **109**, 1492 (1958).
[12] H. Cao, Opt. Photonics News **16**, 24 (2005).
[13] S. Mujumdar, M. Ricci, R. Torre, and D. S. Wiersma, Phys. Rev. Lett. **93**, 053903 (2004).
[14] G. Zacharakis, N. A. Papadogiannis, G. Filippidis, and T. G. Papazoglou, Opt. Lett. **25**, 923 (2000).
[15] L. Florescu and S. John, Phys. Rev. Lett. **93**, 013602 (2004).
[16] H. Cao, Y. Ling, J. Y. Xu, C. Q. Cao, and P. Kumar, Phys. Rev. Lett. **86**, 4524 (2001).
[17] D. S. Wiersma, Nat. Phys. **4**, 359 (2008).
[18] V. M. Apalkov, M. E. Raikh, and B. Shapiro, Phys. Rev. Lett. **89**, 016802 (2002).
[19] P. D. García, M. Ibisate, R. Sapienza, D. S. Wiersma, and C. López, Phys. Rev. A **80**, 013833 (2009).
[20] J. Yi, G. Feng, L. Yang, K. Yao, C. Yang, Y. Song, and S. Zhou, Opt. Commun. **285**, 5276 (2012).
[21] D. S. Wiersma and S. Cavalieri, Nature **414**, 708 (2001).
[22] D. S. Wiersma and S. Cavalieri, Phys. Rev. E **66**, 056612 (2002).
[23] S. Ferjani, V. Barna, A. De Luca, C. Versace, N. Scaramuzza, R. Bartolino, and G. Strangi, Appl. Phys. Lett. **89**, 121109 (2006).
[24] Q. Song, S. Xiao, X. Zhou, L. Liu, L. Xu, Y. Wu, and Z. Wang, Opt. Lett. **32**, 373 (2007).
[25] Q. Song, L. Liu, L. Xu, Y. Wu, and Z. Wang, Opt. Lett. **34**, 298 (2009).
[26] C. R. Lee, J. D. Lin, B. Y. Huang, S. H. Lin, T. S. Mo, S. Y. Huang, C. T. Kuo, and H. C. Yeh, Opt. Express **19**, 2391 (2011).
[27] S. Diez, D. O. López, M. R. de la Fuente, M. A. Pérez-Jubindo, J. Salud, and J. Ll. Tamarit, J. Phys. Chem. B **109**, 23209 (2005).
[28] M. A. Pérez-Jubindo, M. R. de la Fuente, S. Diez-Berart, D. O. López, and J. Salud, J. Phys. Chem. B **112**, 6567 (2008).
[29] M. R. de la Fuente, D. O. López, M. A. Pérez-Jubindo, D. A. Dunmur, S. Diez-Berart, and J. Salud, J. Phys. Chem. B **114**, 7864 (2010).
[30] M. B. Sied, J. Salud, D. O. López, M. Barrio, and J. Ll. Tamarit, Phys. Chem. Phys. Chem. **4**, 2587 (2002).
[31] *Series on Directions in Condensed Matter Physics: Scattering and Localization of Classical Waves in Random Media*, edited by P. Sheng (World Scientific, Singapore, 1990), Vol. 8, Chap. 2.
[32] D. L. Uhrich, V. O. Aimiuwu, P. I. Ktorides, and W. Laprice, Phys. Rev. A **12**, 211 (1975).
[33] J. Doucet and A. Levelut, J. Phys. **38**, 1163 (1977).
[34] K. L. Lushington, G. B. Kasting, and C. W. Garland, J. Phys. (Paris), Lett. **41**, L419 (1980).
[35] W. J. Laprice and D. L. Uhrich, J. Chem. Phys. **72**, 678 (1980).
[36] E. Juszynska, M. Jasiurkowska, M. Massalka-Arodz, D. Takajo, and A. Inaba, Mol. Cryst. Liq. Cryst. **540**, 127 (2011).
[37] J. Salud, D. O. López, S. Diez-Berart, and M. R. de la Fuente, Liq. Cryst. **40**, 293 (2013).
[38] T. Zhai, Y. Zhou, S. Chen, Z. Wang, J. Shi, D. Liu, and X. Zhang, Phys. Rev. A **82**, 023824 (2010).
[39] J. Hernsdorf, B. Guilhabert, Y. Chen, A. Mackintosh, R. Pethrick, P. Skabara, E. Gu, N. Laurand, and M. D. Dawson, Opt. Express **18**, 25535 (2010).
[40] Y. Chen, J. Hernsdorf, B. Guilhabert, Y. Zhang, I. M. Watson, E. Gu, N. Laurand, and M. D. Dawson, Opt. Express **19**, 2996 (2011).
[41] D. S. Wiersma, M. P. van Albada, and A. Lagendijk, Rev. Sci. Instrum. **66**, 5473 (1995).
[42] M. B. van der Mark, M. P. van Albada, and A. Lagendijk, Phys. Rev. B **37**, 3575 (1988).
[43] E. Akkermans and G. Montambaux, *Mesoscopic Physics of Electrons and Photons* (Cambridge University Press, Cambridge, 2007), Chap. 8.
[44] A. Lagendijk, B. Vreeker, and P. de Vries, Phys. Lett. A **136**, 81 (1989); I. Freund and R. Berkovits, Phys. Rev. B **41**, 496 (1990).
[45] J. X. Zhu, D. J. Pine, and D. A. Weitz, Phys. Rev. A **44**, 3948 (1991).
[46] D. S. Wiersma, M. P. van Albada, B. A. van Tiggelen, and A. Lagendijk, Phys. Rev. Lett. **74**, 4193 (1995).
[47] H. Cao, Waves Random Media **13**, R1 (2003).